FUNDAMENTAL ANALYSIS OF THE SYNCHRONOUS GENERATOR – TCSC SYSTEM USING THE ICAD FRAMEWORK

Carlos Ugalde Enrique Acha
University of Glasgow
Glasgow, Scotland, UK
C.Ugalde@elec.gla.ac.uk E.Acha@elec.gla.ac.uk

Eduardo Licéaga-Castro
Universidad Carlos III
Madrid, Spain
edcastro@ing.uc3m.es

Luigi Vanfretti
Rensselaer Polytechnic Institute
Troy, NY, USA
vanfrl@rpi.edu

Abstract – The TCSC, a mature member of the FACTS technology, is the electronically-controlled counterpart of the conventional series bank of capacitors. Its major benefits are its ability to regulate power flows along the compensated line and to rapidly modulate its effective impedance. In this paper, fundamental analysis of the synchronous generator – TCSC system using Individual Channel Analysis and Design, is carried out. The main benefits of this approach in control system design tasks are elucidated. Fundamental analysis is used to explain the generator dynamic behaviour as affected by the TCSC. The system is modelled as a 3x3 multivariable plant. Moreover, a control system design for the system is presented, with particular emphasis in the closed-loop performance and stability and structural robustness assessment. The percentage of series compensation is varied (50, 25 and 10%) by changing the firing angle of the TCSC. It is formally shown that the addition of the TCSC improves the dynamical performance of the synchronous machine by substantially decreasing the electrical distance and therefore considerably reducing the awkward switch-back characteristic exhibited by synchronous generators. However, the TCSC inclusion brings on fragility to the global system, making it non-minimum phase and introducing adverse dynamics in the speed channel of the synchronous machine.

Keywords: TCSC, synchronous generator, individual channel analysis and design, stability, robustness

1 INTRODUCTION

Active power transfers between areas may be substantially increased and adjusted very effectively by varying the net series impedance of the series compensated line. The Thyristor-Controlled Series Compensator (TCSC), an already installed and mature member of the second generation of FACTS devices, is the electronically-controlled counterpart of the conventional series bank of capacitors [1]. Its major benefits are its ability to regulate power flows along the compensated line and to rapidly modulate the effective impedance of the line in response to dynamic events in the vicinity of the line – allowing a smooth control of transmission line compensation levels. Experience with the operation of TCSC facilities has encouraged power system planners to look at the TCSC as a realistic solution for providing better control in the high-voltage side of the power network [2-4]. This fact provides the motivation to carry out fundamental studies of the dynamic behaviour of transmission systems including TCSC representation. So far, valuable transfer function block-diagram models of the synchronous machine–TCSC system have been developed [5]. Such representation yields physical insight and understanding of the system behaviour. Although it enables a transparent analysis of the interaction between internal variables in terms of constants and transfer functions that fully encapsulate all key dynamic parameters, not all interactions between the various variables may be useful for control system design purposes.

A successful integration of FACTS devices into power systems networks is of great importance for all sectors of the market: power generation, transmission, distribution, and high-voltage power electronics equipment manufacturers. The proper understanding of the TCSC will positively contribute to this task. However, further research is required as the existing analysis tools, although applicable to large-scale systems, lack physical transparency [6].

Individual Channel Analysis and Design (ICAD) provides an alternative and very insightful control-oriented framework with which to carry out small-signal stability assessments. In this paper dynamic studies of the synchronous generator–TCSC system using ICAD are reported for the first time. A comprehensive description of the basic methodology can be found in [7,8]. Throughout the analysis of Multivariable Structure Functions (MSF), the dynamical behaviour and structure of the system can be described in a global context. Moreover, ICAD allows analysis and synthesis of multivariable control design with the possibility of an assessment of the robustness and performance of the control system. The synchronous generator – TCSC system can be modelled as a 3x3 plant. Its performance is evaluated using ICAD, illustrating the great benefits of this approach. Fundamental analysis is carried out explaining the generator dynamic behaviour as affected by the TCSC.

2 SYSTEM UNDER STUDY

The synchronous machine dynamic representation used to derive the model presented here is based on the work of Hammons and Winning [9]. The test system under study (figure 1) is used to assess the influence that the TCSC exerts on the generator dynamic characteristic. It consists of one synchronous generator feeding into an infinite-bus system via a TCSC compensated tie-line. A synchronous machine of 6 *p.u.* on a base power of 100 *MVA* is considered, with parameters given as in [5].

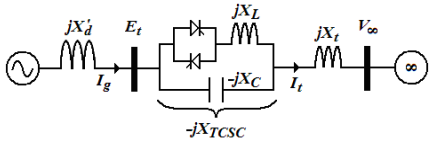

Figure 1: Synchronous generator – TCSC system.

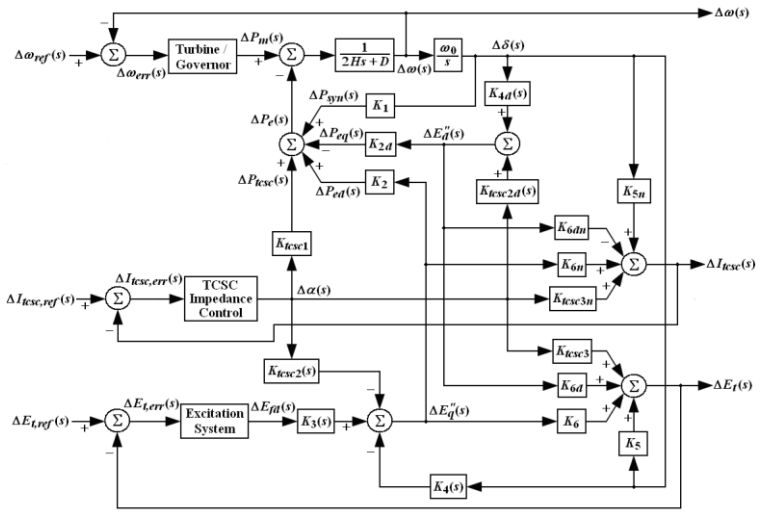

Figure 2: Detailed block diagram for a synchronous generator – TCSC system including controllers.

2.1 Block Diagram Representation

The small-signal model is developed from first principles, by using the non-linear and algebraic equations that represent the synchronous generator and the TCSC. In order to study the dynamic interaction between the generator and the TCSC, the effects of the field and damping windings in the *d* and *q*-axes should be included. Therefore, a 5th order salient-pole synchronous generator model is considered, which accounts for the effects of the generator main field winding plus one damper winding in the *d*-axis and one in the *q*-axis. After manipulating the relevant transfer-function expressions, in the *s*-domain, the following linearised equations are arrived at [5]:

$$\Delta P_e(s) = K_1\Delta\delta(s) + K_2\Delta E_q^{"}(s) - K_{2d}\Delta E_d^{"}(s) + K_{TCSC1}\Delta\alpha(s)$$

$$\Delta E_t(s) = K_5\Delta\delta(s) + K_6\Delta E_q^{"}(s) + K_{6d}\Delta E_d^{"}(s) + K_{TCSC3}\Delta\alpha(s)$$

$$\Delta I_{TCSC}(s) = K_{5n}\Delta\delta(s) + K_{6n}\Delta E_q^{"}(s) - K_{6dn}\Delta E_d^{"}(s) + K_{TCSC3n}\Delta\alpha(s)$$

$$\Delta E_q^{"}(s) = K_3(s)\Delta E_{fd}(s) - K_4(s)\Delta\delta(s) - K_{TCSC2}(s)\Delta\alpha(s)$$

$$\Delta E_d^{"} = K_{4d}(s)\Delta\delta + K_{TCSC2d}(s)\Delta\alpha(s)$$

$$\Delta\omega(s) = (1/2Hs)\cdot\left[\Delta P_m(s) - \Delta P_e(s) - D\Delta\omega(s)\right]$$

$$\Delta\delta(s) = (\omega_0/s)\Delta\omega(s)$$

The previous equations (whose parameters can be found in reference [5]) are used to form the block diagram representation shown in figure 2. It can be seen that there are 3-input 3-output feedback subsystems in the generator – TCSC block diagram, *i.e.*, excitation, turbine-governor and TCSC impedance control loops. These are in addition to the generator TCSC – system, whose outputs of interest are generator speed ($\Delta\omega$), generator output voltage (ΔE_t) and TCSC current (ΔI_{TCSC}) flowing through the tie line.

The block diagram of the generator – TCSC system yields unique physical insight as to how the TCSC dynamically affects the generator. It enables a transparent analysis of the interaction between internal machine variables and the TCSC in terms of constants and transfer functions that encapsulate fully all key dynamic parameters of the system. However, caution needs to be exercised since not all interactions between the various variables may be useful for control system design purposes. Such ambiguities can be avoided by working with the alternative control-oriented framework termed ICAD, a powerful analysis and design tool which is well suited to the task of carrying out small signal stability assessments. The dynamical behaviour and structure of the system can be described in a global context in which the characteristics of the individual transfer functions do not have a primordial relevance.

2.2 TCSC Characteristic

The TCSC is connected in series with the tie-line, as shown in figure 1. The active power flow can be adjusted by controlling the TCSC impedance (X_{TCSC}). This is achieved by suitably changing the thyristor's firing angle. The expression for the fundamental frequency of the TCSC impedance, as a function of the thyristor's firing angle, is given as [10]:

$$X_{TCSC} = -X_C + C_1\left\{2(\pi-\alpha) + \sin\left[2(\pi-\alpha)\right]\right\} + \\ -C_2\cos^2(\pi-\alpha)\left\{\lambda\tan\left[\lambda(\pi-\alpha)\right] - \tan(\pi-\alpha)\right\} \quad (1)$$

For a small variation, the derivative value of the TCSC impedance characteristic, $F(\alpha) = \partial X_{TCSC}/\partial\alpha$, is given by

$$F(\alpha) = -2C_1(1+\cos 2\alpha) + C_2\left\{\frac{\lambda^2\cos^2(\pi-\alpha)}{\cos^2\left[\lambda(\pi-\alpha)\right]} - 1\right\} \quad (2)$$
$$+C_2\sin 2\alpha\left\{\lambda\tan\left[\lambda(\pi-\alpha)\right] - \tan(\pi-\alpha)\right\}$$

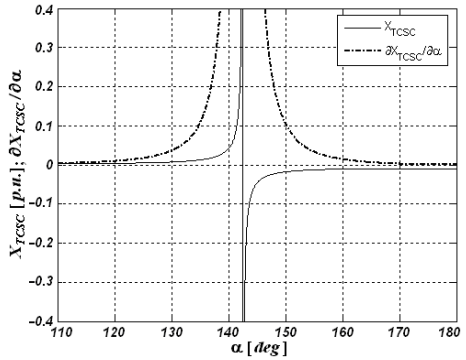

Figure 3: TCSC impedance characteristic (X_{TCSC}) and its derivative $F(\alpha) = \partial X_{TCSC}/\partial\alpha$ for given parameters.

where

$$C_1 = \frac{X_C + X_{LC}}{\pi} \qquad C_2 = \frac{4X_{LC}^2}{\pi X_L} \qquad \lambda = \frac{\omega_0}{\omega} = \sqrt{\frac{X_C}{X_L}}$$

$$X_{LC} = \frac{X_C X_L}{X_C - X_L} \qquad \omega_0^2 = \frac{1}{LC} = \omega^2 \frac{X_C}{X_L}$$

Consider a TCSC with inductive and capacitive reactance values corresponding to those of the fully operational Kayenta TCSC installation [11]. Figure 3 shows the fundamental frequency reactance as a function of α and its derivative $F(\alpha)$.

From figure 3 it can be observed that the impedance characteristic has two distinctive regions of operation, one inductive and one capacitive, as the TCSC firing angle increases. The capacitive region starts at a firing angle of approximately 142.6°. For firing angle values near the resonant point the variations of X_{TCSC} are quite large even for a small variation in the controlling firing angle. If an increase of TCSC impedance in the capacitive mode is required then the firing angle value should move towards the resonant point. Also, $F(\alpha)$ has always negative values in the TCSC firing angle range. The effect of $F(\alpha)$ appears in many of the system coefficients of the block-diagram model.

2.3 Transfer Matrix Representation

The transfer matrix representation of the system is not only desirable but essential for the analysis of the synchronous generator – TCSC plant dynamics under the ICAD framework. After some arduous algebraic manipulation, such representation is obtained, given by

$$\begin{bmatrix} \Delta\omega(s) \\ \Delta E_t(s) \\ \Delta I_{TCSC}(s) \end{bmatrix} = \begin{bmatrix} g_{11}(s) & g_{12}(s) & g_{13}(s) \\ g_{21}(s) & g_{22}(s) & g_{23}(s) \\ g_{31}(s) & g_{32}(s) & g_{33}(s) \end{bmatrix} \begin{bmatrix} \Delta P_m(s) \\ \Delta E_{fd}(s) \\ \Delta\alpha(s) \end{bmatrix} \qquad (3)$$

or in a more compact form as

$$\mathbf{y}(s) = \mathbf{G}(s)\mathbf{u}(s) \qquad (4)$$

where $\mathbf{G}(s)$ is the transfer matrix of the 3x3 linearised model of the synchronous generator – TCSC system.

For control system analysis, the closed-loop diagram of the system is shown in figure 4.

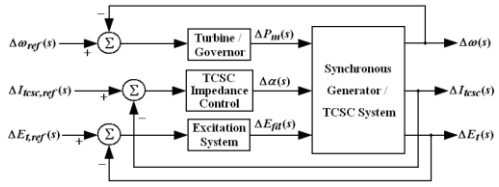

Figure 4: Block diagram of closed-loop system.

A complete study case is carried out in this paper. It assesses the influence that the TCSC exerts on the generator dynamic characteristic when the tie-line reactance has a fixed value (X_t = 0.4 *p.u.*) and the percentage of series compensation is varied (50, 25, 10%) by changing the firing angle α. At a later stage, a performance comparison between a system with no TCSC and one with TCSC is made. Provided the operating conditions (not included in the paper), it is important to mention that numerical calculation shows that all individual elements $g_{ij}(s)$ in (3) are stable and minimum-phase.

3 MULTIVARIABLE ANALYSIS

In the framework afforded by ICAD, the dynamical structure of plant (3) is determined by input-output channels resulting from pairing each input to each output by means of diagonal controllers. For the case of the synchronous generator – TCSC system, the traditional pairing of inputs to outputs is given as [5]

$$\mathbf{K}(s) = \begin{bmatrix} k_1 & 0 & 0 \\ 0 & k_2 & 0 \\ 0 & 0 & k_3 \end{bmatrix} \Rightarrow \begin{cases} C_1(s): \Delta P_m(s) \rightarrow \Delta\omega(s) \\ C_2(s): \Delta E_{fd}(s) \rightarrow \Delta E_t(s) \\ C_3(s): \Delta\alpha(s) \rightarrow \Delta I_{TCSC}(s) \end{cases} \qquad (5)$$

The diagonal controller given in (5), which considers pairings as $\Delta P_m(s) \rightarrow \Delta\omega(s)$, $\Delta E_{fd}(s) \rightarrow \Delta E_t(s)$ and $\Delta\alpha(s) \rightarrow \Delta I_{TCSC}(s)$, agrees with that used for conventional controllers and this would be the only case considered in this paper. Coupling between channels is determined by Multivariable Structure Functions (MSF) $\Gamma_i(s)$ [8], which are indicators of the potential performance of feedback control. A small magnitude of MSF is amenable to a low signal interaction between channels.

The MSFs $\Gamma_i(s)$, i = 1,2, are defined as

$$\Gamma_i(s) = -\left|\mathbf{G}_i^{12\ldots(i-1)}\right| / g_{ii} \left|\mathbf{G}^{12\ldots(i-1)i}\right| \qquad (6)$$

where $\mathbf{G}^{i_1 i_2 \ldots i_r}$ is the transfer function matrix obtained from the plant matrix $\mathbf{G}(s)$ by eliminating rows and columns of elements i_1, i_2, …, i_r; and matrix $\mathbf{G}_j^{i_1 i_2 \ldots i_r}$ is the transfer function matrix obtained from $\mathbf{G}(s)$ by setting diagonal element g_{jj} of $\mathbf{G}(s)$ to zero before eliminating the rows and columns as in the definition of $\mathbf{G}^{i_1 i_2 \ldots i_r}$.

It should be noted that all MSFs associated to the model share some important common characteristics for the study. Numerical calculation shows that they are stable and minimum-phase. Moreover, their Nyquist plots (not included) start to the left of the point (1,0). Such features ease the design process. After suitable analysis of the MSFs associated to the 3x3 system, the following can be said about the channels:

- Multiple Channel $\mathbf{M}_{23}(s)$ is highly coupled with Individual Channel $C_1(s)$ – increase of series compensation decreases coupling. Channels $C_2(s)$ and $C_3(s)$ are lightly coupled – increase of series compensation increases coupling.
- $\mathbf{M}_{13}(s)$ is lowly coupled with $C_2(s)$ – increase of compensation increases coupling. Channels $C_1(s)$ and $C_3(s)$ are highly coupled – increase of compensation decreases coupling.
- $\mathbf{M}_{12}(s)$ is highly coupled with $C_3(s)$ – increase of compensation decreases coupling. Channels $C_1(s)$ and $C_2(s)$ are lowly coupled – increase of compensation decreases coupling.

It can be safely stated that the TCSC together with the synchronous machine, regardless of the amount of series compensation and tie-line reactance value, produces a highly coupled multivariable system – particularly at low frequencies over the range of interest of 1–10 *rad/s*. It should be noted that the TCSC impedance control loop, represented by $C_3(s)$, tends to significantly couple with the speed channel of the synchronous generator, *i.e.*, $C_1(s)$.

Within the ICAD context, Multiple Channel $\mathbf{M}_{12}(s)$ represents the actual dynamics of the synchronous generator under the influence of the TCSC. It has been known and formally proven using ICAD [12] that for long-distance transmission system operation becomes impaired because of the long electrical distances involved. Previous results obtained while considering a synchronous generator with no TCSC show that coupling within the machine is low under a lagging power factor operation; in fact, channel coupling increases with electrical distance, decreasing stability robustness [12]. The latter conclusion is further confirmed in this paper.

The previous analysis is important since it may dictate a control design strategy. For instance, as coupling in Multiple Channel $\mathbf{M}_{12}(s)$ is low, it can be designed independently of Individual Channel $C_3(s)$. Considering a rearranged transfer matrix

$$\begin{bmatrix} \Delta I_{TCSC}(s) \\ \Delta\omega(s) \\ \Delta E_t(s) \end{bmatrix} = \begin{bmatrix} g_{33}(s) & g_{31}(s) & g_{32}(s) \\ g_{13}(s) & g_{11}(s) & g_{12}(s) \\ g_{23}(s) & g_{21}(s) & g_{22}(s) \end{bmatrix} \begin{bmatrix} \Delta\alpha(s) \\ \Delta P_m(s) \\ \Delta E_{fd}(s) \end{bmatrix} \tag{7}$$

the following partitioned system is used for design:

$$\mathbf{G}(s) = \begin{bmatrix} \mathbf{G}_{11}(s) & \mathbf{G}_{12}(s) \\ \mathbf{G}_{21}(s) & \mathbf{G}_{22}(s) \end{bmatrix} \quad \mathbf{K}(s) = \begin{bmatrix} \mathbf{K}_1(s) & \mathbf{0} \\ \mathbf{0} & \mathbf{K}_2(s) \end{bmatrix} \tag{8}$$

$$\mathbf{r}(s) = \begin{bmatrix} \mathbf{r}_1(s) \\ \mathbf{r}_2(s) \end{bmatrix} \qquad \mathbf{y}(s) = \begin{bmatrix} \mathbf{y}_1(s) \\ \mathbf{y}_2(s) \end{bmatrix} \tag{9}$$

where

$$\mathbf{G}_{11}(s) = g_{33}(s) \qquad \mathbf{G}_{12}(s) = \begin{bmatrix} g_{31}(s) & g_{32}(s) \end{bmatrix}$$

$$\mathbf{G}_{21}(s) = \begin{bmatrix} g_{13}(s) \\ g_{23}(s) \end{bmatrix} \qquad \mathbf{G}_{22}(s) = \begin{bmatrix} g_{11}(s) & g_{12}(s) \\ g_{21}(s) & g_{22}(s) \end{bmatrix}$$

$$\mathbf{r}_1(s) = r_3(s);\ \mathbf{r}_2(s) = \begin{bmatrix} r_1(s) \\ r_2(s) \end{bmatrix};\ \mathbf{y}_1(s) = y_3(s);\ \mathbf{y}_2(s) = \begin{bmatrix} y_1(s) \\ y_2(s) \end{bmatrix}$$

$$\mathbf{K}_1(s) = k_3(s) \qquad \mathbf{K}_2(s) = \begin{bmatrix} k_1(s) & 0 \\ 0 & k_2(s) \end{bmatrix}$$

Individual Channel $C_3(s)$ is expressed by

$$\begin{aligned} \mathbf{M}_1(s) = C_3(s) &= \left(\mathbf{I} - \mathbf{G}_{12}\mathbf{G}_{22}^{-1}\mathbf{H}_2\mathbf{G}_{21}\mathbf{G}_{11}^{-1}\right)\mathbf{G}_{11}\mathbf{K}_1 \\ &= k_3 g_{33}(s)\left(1 - \mathbf{G}_{12}(s)\mathbf{G}_{22}^{-1}(s)\mathbf{H}_2(s)\mathbf{G}_{21}(s)g_{33}^{-1}(s)\right) \end{aligned} \tag{10}$$

where the multiple subsystem transfer function matrix $\mathbf{H}_2(s)$ is given by

$$\mathbf{H}_2(s) = \mathbf{G}_{22}(s)\mathbf{K}_2(s)\left(\mathbf{I} + \mathbf{G}_{22}(s)\mathbf{K}_2(s)\right)^{-1} \tag{11}$$

and is subjected to the cross-reference disturbance

$$\mathbf{D}_1(s) = \mathbf{G}_{12}(s)\mathbf{G}_{22}^{-1}(s)\mathbf{H}_2(s) \tag{12}$$

Multiple Channel $\mathbf{M}_{12}(s)$ is expressed by

$$\begin{aligned} \mathbf{M}_2(s) = \mathbf{M}_{12}(s) &= \left(\mathbf{I}_{2x2} - \mathbf{G}_{21}\mathbf{G}_{11}^{-1}\mathbf{H}_1\mathbf{G}_{12}\mathbf{G}_{22}^{-1}\right)\mathbf{G}_{22}\mathbf{K}_2 \\ &= \left(\mathbf{I}_{2x2} - g_{33}^{-1}(s)h_1(s)\mathbf{G}_{21}(s)\mathbf{G}_{12}(s)\mathbf{G}_{22}^{-1}(s)\right)\mathbf{G}_{22}\mathbf{K}_2 \end{aligned} \tag{13}$$

where $\mathbf{H}_1(s)$ is given by

$$\mathbf{H}_1(s) = h_1(s) = k_3(s)g_{33}(s)\left(1 + k_3(s)g_{33}(s)\right)^{-1} \tag{14}$$

and is subjected to the cross-reference disturbance

$$\mathbf{D}_2(s) = g_{33}^{-1}(s)h_1(s)\mathbf{G}_{21}(s) \tag{15}$$

Assuming $h_1(s) = 1$, Multiple Channel $\mathbf{M}_{12}(s)$ is designed as a separate $2x2$ system. Once controllers $k_1(s)$ and $k_2(s)$ are obtained, $\mathbf{H}_2$ can be defined (that is, the interaction of $\mathbf{M}_{12}(s)$ with $C_3(s)$) and a controller $k_3(s)$ for Individual Channel $C_3(s)$ as indicated in equation (10) can be designed. After that, an expression for $h_1(s)$ (interaction with $\mathbf{M}_{12}(s)$) is calculated and controllers $k_1(s)$ and $k_2(s)$ are re-designed. The process is repeated until a successful multivariable controller is achieved for all channels and robustness is assured in each individual channel, subsystems $\mathbf{H}_i(s)$, and MSFs $\gamma_i(s)$.

4 CONTROL SYSTEM DESIGN EXAMPLE

After analysing the MSFs and transfer matrix associated to the model, the following diagonal controller

$$\begin{aligned} \mathbf{K}_1(s) &= \begin{bmatrix} k_1(s) & 0 & 0 \\ 0 & k_2(s) & 0 \\ 0 & 0 & k_3(s) \end{bmatrix} \\ &= \operatorname{diag}\left[\frac{5.75\left(s^2 + 6.1s + 165.5\right)}{s^2(s+5)},\ \frac{14(s+0.43)}{s},\ -\frac{k_{TCSC}(s+0.2)}{s(s+7)(s+0.7)} \right] \end{aligned} \tag{16}$$

was obtained, where k_{TCSC} is a scalar gain for the TCSC impedance control loop which varies according to the level of compensation; for instance, $k_{TCSC} = -1$ for 50%, –2 for 25% and –16 for 10% of compensation. The control system performance and stability robustness indicators are presented in figures 5–8.

From figures 5–8, it can be seen that the control system performance is adequate for all operating conditions as controller (16) successfully decouples the generator channels for typical frequencies [13] and the speed regulation is effective for lower frequency signals, blinding interaction with higher frequency terminal voltage and TCSC impedance control channels. However, performance tends to improve whenever the amount of series compensation provided by the TCSC is increased. Furthermore, stability and structural robustness measures are higher with an increase of compensation. Notice that gains k_{TCSC} of the impedance control loop in (16) are chosen in such a way that the bandwidths of the individual channels are maintained regardless of the amount of compensation while still providing adequate robustness margins, *i.e.*, gain and phase margins over 6 *dB* and 40 *deg*, respectively [13].

Remarks: Although performance seems to be adequate, it is of great importance to notice that channel $C_3(s)$ is non-minimum phase. In fact, it can be seen from figure 8 that $\gamma_3(s)$ circles the point (1,0) twice in clockwise direction for all operating conditions. Such a situation poses a major inconvenience for control system design and limits the system performance. Even under disturbances, the bandwidth of $C_3(s)$ should be kept low and below the values of the unstable zero pair; otherwise, instability might arise.

It should also be mentioned that diagonal controller (16), by including an integral action in each of its individual elements, guarantees a high gain at low frequencies and a zero steady-state error. The extra lead zero-pole pair in $k_3(s)$ is used to increase stability margins.

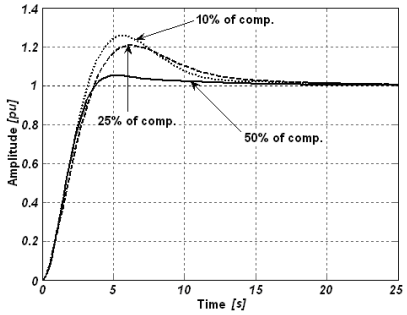

(*a*)

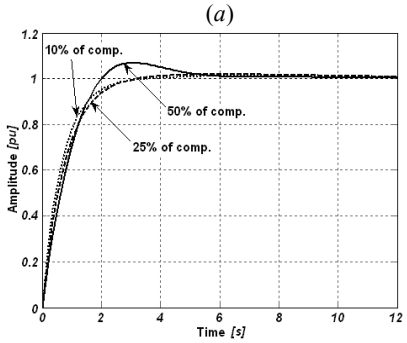

(*b*)

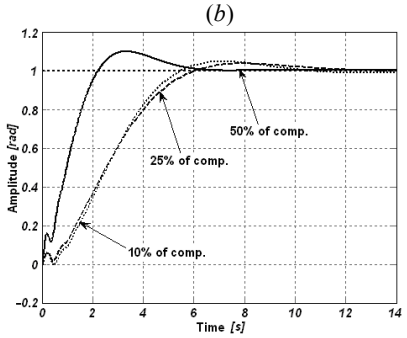

(*c*)

Figure 5: System Performance. Step Response of: (*a*) Channel 1 $T_{c1}(s)$; (*b*) Channel 2 $T_{c2}(s)$; (*c*) Channel 3 $T_{c3}(s)$

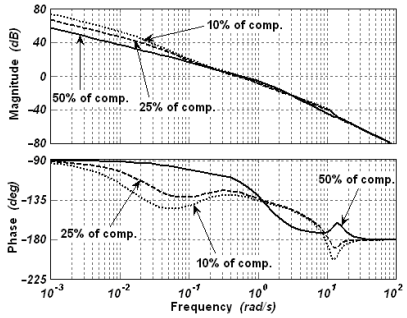

(*a*)

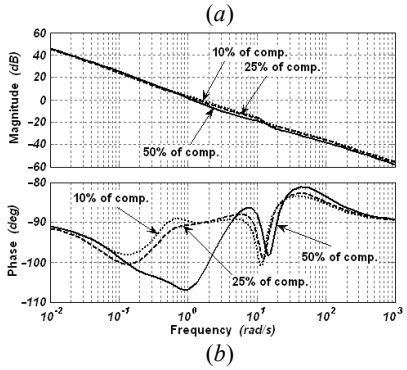

(*b*)

Figure 6: System performance and stability robustness assessment. Bode diagrams: (*a*) Channel 1 $C_1(s)$; (*b*) Ch. 2 $C_2(s)$

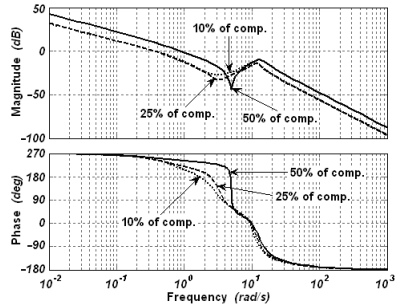

(*c*)

Figure 6: System performance and stability robustness assessment. Bode diagrams: (*c*) Channel 3 $C_3(s)$

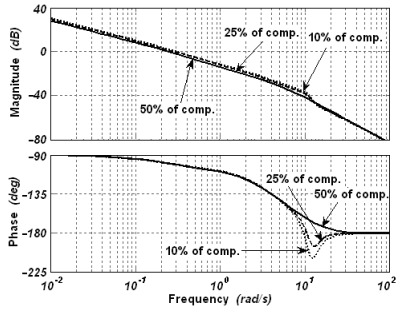

(*a*)

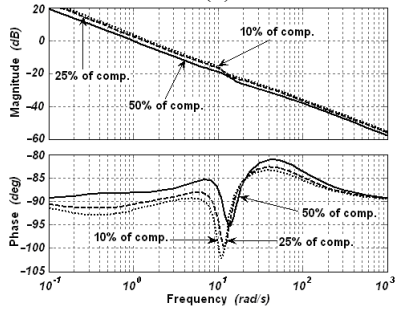

(*b*)

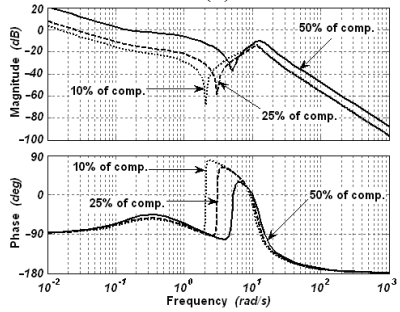

(*c*)

Figure 7: Stability robustness assessment. Bode diagrams of: (*a*) $k_1 g_{11}(s)$; (*b*) $k_2 g_{22}(s)$; (*c*) $k_3 g_{33}(s)$

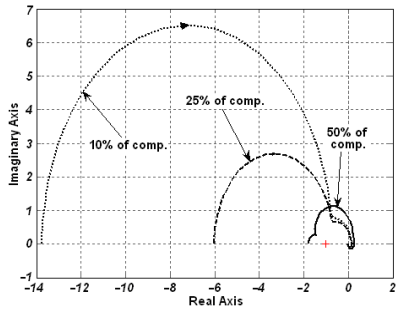

(*a*)

Figure 8: Structural robustness assessment. Nyquist diagrams of: (*a*) $\gamma_1(s)$

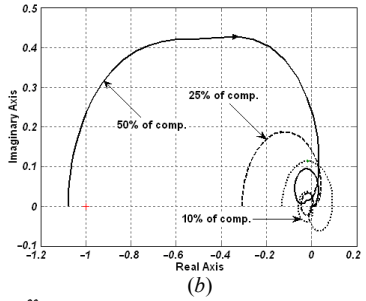

(*b*)

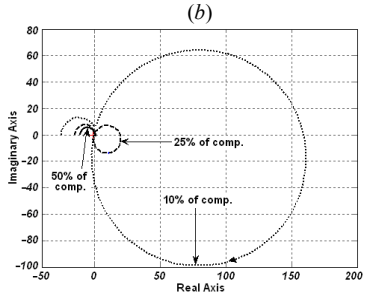

(*c*)

Figure 8: Structural robustness assessment. Nyquist diagrams of: (*b*) $\gamma_2(s)$; (*c*) $\gamma_3(s)$

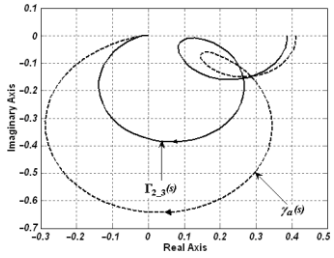

(*a*)

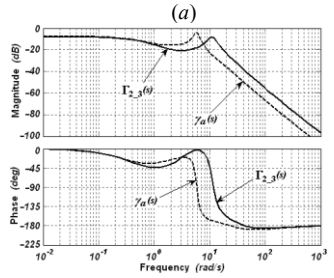

(*b*)

Figure 9: $\gamma_a(s)$ vs $\Gamma_{2\_3}(s)$. (*a*) Nyquist plot; (*b*) Bode plot

5 TCSC INFLUENCE ON THE SYSTEM

The control system characteristics are investigated to show the influence that the TCSC exerts on the system. The TCSC is used to decrease the electrical length of the transmission line in order to boost active power transfer. A high value of tie-line reactance $X_t = 0.6$ *p.u.* is considered. When in operation, the TCSC provides a 33.33% of series compensation ($X_{TCSC} = -0.2$ *p.u.*).

Figure 9 shows the relevant MSFs with and with no presence of TCSC. $\Gamma_{2\_3}(s)$ gives a measure of coupling between channels of the synchronous generator ($C_1(s)$, speed, and $C_2(s)$, voltage) in Multiple Channel $\mathbf{M}_{12}(s)$ when a TCSC is used. On the other hand, $\gamma_a(s)$ provides the coupling measure for the synchronous generator when no TCSC is considered. It can be seen that both $\Gamma_{2\_3}(s)$ and $\gamma_a(s)$ have a similar frequency response – that is, the dynamical structure is preserved. However, coupling is significantly lower and the structural robustness measures (in terms of gain and phase margins) increase whenever the TCSC is used. Notice how the frequency peak in magnitude is translated to higher frequencies by including the TCSC.

The performance of the synchronous generator is compared to that obtained for the system including one TCSC. A controller for the 2*x*2 system without considering the TCSC channel is considered, that is

$$\mathbf{K}_1(s) = \mathrm{diag}\left[\frac{5.75\left(s^2+6.1s+165.5\right)}{s^2(s+5)} \quad \frac{14(s+0.43)}{s}\right] \quad (17)$$

Notice that controller (17) is exactly the same as (16) without the TCSC channel. When the TCSC is used, $k_{TCSC} = -1/2$ in the impedance control loop. Figures 10–12 show the performance of the closed-loop control system (terminal voltage and speed channels) and robustness assessment with and with no TCSC.

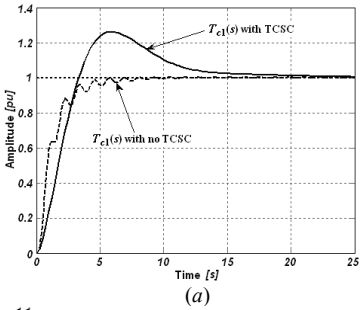

(*a*)

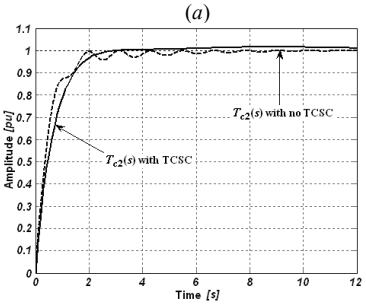

(*b*)

Figure 10: System performance with and with no TCSC. Step Response of: (*a*) Channel 1 $T_{c1}(s)$; (*b*) Channel 2 $T_{c2}(s)$

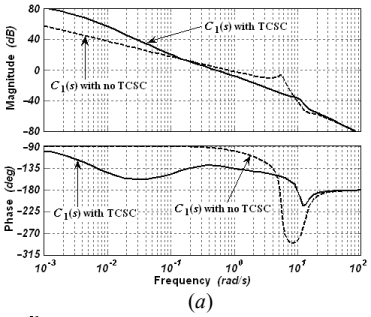

(*a*)

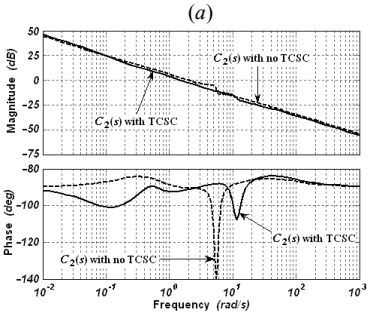

(*b*)

Figure 11: System performance and robustness assessment with and with no TCSC. Bode diagrams: (*a*) $C_1(s)$; (*b*) $C_2(s)$

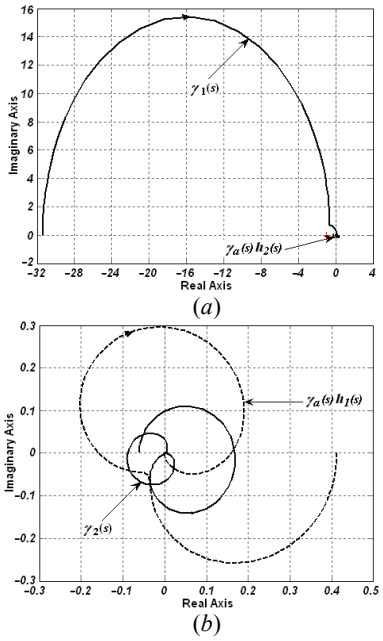

Figure 12: Structural robustness assessment with and with no TCSC. Nyquist diagrams: $(a)\gamma_a h_2(s)$ *vs* $\gamma_1(s)$;(b) $\gamma_a h_1(s)$ *vs* $\gamma_2(s)$

From figure 10, it can be seen that the system tends to be oscillatory whenever the TCSC is not used. However, the Bode diagram of $C_1(s)$ in figure 11 shows an important effect that the TCSC causes in the system: stability robustness decreases – which is a proof that $C_3(s)$ significantly couples with the speed channel $C_1(s)$. However, an important positive effect of the inclusion of the TCSC can be appreciated in the Bode diagram of $C_2(s)$ shown in figure 11: the switch-back characteristic, quite prominent with no TCSC reduces very considerably and moves on to higher frequencies whenever the TCSC is used. Also, the use of the TCSC considerably improves structural robustness in the voltage channel $C_2(s)$, but tends to worsen the speed channel $C_1(s)$ (figure 12).

6 CONCLUSION

In this paper a small-signal stability assessment and control system analysis and design of the synchronous generator – TCSC system has been carried out. The parameters of the fully operational and already installed TCSC in Kayenta have been considered. By means of the ICAD framework, fundamental analyses have been carried out explaining the generator dynamics as affected by the TCSC. Simulation results obtained are in agreement with system behaviour observed in practice.

It is formally shown that the addition of the TCSC improves the dynamical performance of the synchronous machine by decreasing the electrical distance and therefore considerably reducing the awkward switch-back characteristic. Although an effective modulation of the tie-line reactance and a better regulation of the power flows are available, it should be noticed that the inclusion of a TCSC brings fragility to the global system because of two main reasons: the system becomes non-minimum phase, limiting the potential performance; and the TCSC impedance control loop introduces adverse dynamics in terms of cross-coupling, particularly to the speed channel of the synchronous machine.

These key points of TCSC operation have been elucidated only after application of ICAD and may not be revealed, at least not as emphatically, by other analysis methods such as block diagram representations and eigenanalysis. Work is under way to develop multi-machine system analysis. Although the complexity and volume of information will substantially increase due to the geometric growth of channel interactions, ICAD can overcome such problems by prioritising the most relevant, *i.e.*, stronger, interactions between machine's channels. One has to be aware that numerical instabilities may arise when dealing with large power systems, but this is not a problem confined to ICAD but to any method that uses transfer function matrices. ICAD is a promising analysis tool for multi-machine power systems.

REFERENCES

[1] IEEE/CIGRE, "FACTS Overview", Special Issue, 95-TP-108, IEEE Service Centre, NJ, USA, 1995.

[2] G. Jancke, N. Fahlen and O. Nerf, "Series Capacitor in Power System", IEEE Trans. Power Apparatus and Systems, 94, pp. 915-925, May 1975.

[3] F. Iliceto and E. Cinieri, "Comparative Analysis of Series and Shunt Compensation Control Schemes for AC Transmission Systems", IEEE Trans. Power Apparatus and Systems, 96(1), pp. 1819-1830, November 1977.

[4] L. Angquist, B. Lundin and J. Samuelsson, "Power Oscillation Damping Using Controlled Reactive Power Compensation: A Comparison between Series and Shunt Approaches", IEEE Trans. Power Systems, 8(2), pp. 687-699, May 1993.

[5] P. Aree, "Small-signal Stability Modelling and Analysis of Power Systems with Electronically Controlled Compensation", PhD Thesis, Department of Electronics and Electrical Engineering, University of Glasgow, Scotland, UK, 2000.

[6] P. Kundur, G.J. Rogers, D.Y. Wong, L. Wang and M.G. Lauby, "A Comprehensive Computer Program Package for Small Signal Stability Analysis of Power Systems", IEEE Trans. on Power Systems, 5(4), pp. 1076-1083, 1990.

[7] J. O'Reilly and W.E. Leithead, "Multivariable Control by Individual Channel Design", International Journal of Control, 54(1), pp. 1-46, 1991.

[8] W.E. Leithead and J. O'Reilly, "*m*-input *m*-output Feedback Control by Individual Channel Design. Part 1. Structural Issues", International Journal of Control, 56(6), pp. 1347-1397, 1992.

[9] T.J. Hammons and D.J. Winning, "Comparisons of Synchronous Machine Models in the Study of the Transient Behaviour of Electrical Power Systems", IEE Proc., 118(10), pp. 1442-1458, 1971.

[10] S.G. Helbing and G.G. Karady, "Investigations of an Advanced Form of Series Compensation", IEEE Trans. Power Delivery, 9(2), pp. 939-947, April 1994.

[11] N. Christl, R. Hedin, K. Sadek, P. Lutzelberger, P.E. Krause, S.M. McKenna, A.H. Montoya and D. Togerson, "Advanced Series Compensation (ASC) with Thyristor Controlled Impedance", Proc. International Conference of Large High Voltage Electric Systems (CIGRE), paper 14/37/38-05, Paris, Sept. 1992.

[12] C.E. Ugalde, L. Vanfretti, E. Liceaga, and E. Acha, "Synchronous Generators Control: from the Traditional Perspective to the ICAD Framework", Proc. International Conference Control 2006 (UK-ACC), Glasgow, Scotland, UK, 2006.

[13] P. Kundur, "Power Systems Stability and Control", The EPRI Power Systems Engineering Series, McGraw-Hill, 1994.